

# World Journal of *Clinical Cases*

*World J Clin Cases* 2021 August 6; 9(22): 6178-6581



**REVIEW**

- 6178 COVID-19 infection and liver injury: Clinical features, biomarkers, potential mechanisms, treatment, and management challenges  
*Sivandzadeh GR, Askari H, Safarpour AR, Ejtehad F, Raeis-Abdollahi E, Vaez Lari A, Abazari MF, Tarkesh F, Bagheri Lankarani K*
- 6201 Gastrointestinal manifestations of systemic sclerosis: An updated review  
*Luquez-Mindiola A, Atuesta AJ, Gómez-Aldana AJ*

**MINIREVIEWS**

- 6218 Mesenchymal stem cell-derived exosomes: An emerging therapeutic strategy for normal and chronic wound healing  
*Zeng QL, Liu DW*
- 6234 Role of autophagy in cholangiocarcinoma: Pathophysiology and implications for therapy  
*Ninfolle E, Pinto C, Benedetti A, Marzioni M, Maroni L*

**ORIGINAL ARTICLE****Case Control Study**

- 6244 Risk factors for intussusception in children with Henoch-Schönlein purpura: A case-control study  
*Zhao Q, Yang Y, He SW, Wang XT, Liu C*

**Retrospective Study**

- 6254 Sequential therapy with combined trans-papillary endoscopic naso-pancreatic and endoscopic retrograde pancreatic drainage for pancreatic pseudocysts  
*He YG, Li J, Peng XH, Wu J, Xie MX, Tang YC, Zheng L, Huang XB*
- 6268 Retrospective study of effect of whole-body vibration training on balance and walking function in stroke patients  
*Xie L, Yi SX, Peng QF, Liu P, Jiang H*
- 6278 Risk factors for preoperative carcinogenesis of bile duct cysts in adults  
*Wu X, Li BL, Zheng CJ, He XD*
- 6287 Diagnostic and prognostic value of secreted protein acidic and rich in cysteine in the diffuse large B-cell lymphoma  
*Pan PJ, Liu JX*
- 6300 Jumbo cup in hip joint renovation may cause the center of rotation to increase  
*Peng YW, Shen JM, Zhang YC, Sun JY, Du YQ, Zhou YG*

**Clinical Trials Study**

- 6308** Effect of exercise training on left ventricular remodeling in patients with myocardial infarction and possible mechanisms  
*Cai M, Wang L, Ren YL*

**Observational Study**

- 6319** Analysis of sleep characteristics and clinical outcomes of 139 adult patients with infective endocarditis after surgery  
*Hu XM, Lin CD, Huang DY, Li XM, Lu F, Wei WT, Yu ZH, Liao HS, Huang F, Huang XZ, Jia FJ*
- 6329** Health-related risky behaviors and their risk factors in adolescents with high-functioning autism  
*Sun YJ, Xu LZ, Ma ZH, Yang YL, Yin TN, Gong XY, Gao ZL, Liu YL, Liu J*
- 6343** Selection of internal fixation method for femoral intertrochanteric fractures using a finite element method  
*Mu JX, Xiang SY, Ma QY, Gu HL*

**META-ANALYSIS**

- 6357** Neoadjuvant chemotherapy for patients with resectable colorectal cancer liver metastases: A systematic review and meta-analysis  
*Zhang Y, Ge L, Weng J, Tuo WY, Liu B, Ma SX, Yang KH, Cai H*

**CASE REPORT**

- 6380** Ruptured intracranial aneurysm presenting as cerebral circulation insufficiency: A case report  
*Zhao L, Zhao SQ, Tang XP*
- 6388** Prostatic carcinosarcoma seven years after radical prostatectomy and hormonal therapy for prostatic adenocarcinoma: A case report  
*Huang X, Cai SL, Xie LP*
- 6393** Pyogenic arthritis, pyoderma gangrenosum, and acne syndrome in a Chinese family: A case report and review of literature  
*Lu LY, Tang XY, Luo GJ, Tang MJ, Liu Y, Yu XJ*
- 6403** Malaria-associated secondary hemophagocytic lympho-histiocytosis: A case report  
*Zhou X, Duan ML*
- 6410** Ileal hemorrhagic infarction after carotid artery stenting: A case report and review of the literature  
*Xu XY, Shen W, Li G, Wang XF, Xu Y*
- 6418** Inflammatory myofibroblastic tumor of the pancreatic neck: A case report and review of literature  
*Chen ZT, Lin YX, Li MX, Zhang T, Wan DL, Lin SZ*
- 6428** Management of heterotopic cesarean scar pregnancy with preservation of intrauterine pregnancy: A case report  
*Chen ZY, Zhou Y, Qian Y, Luo JM, Huang XF, Zhang XM*

- 6435** Manifestation of severe pneumonia in anti-PL-7 antisynthetase syndrome and B cell lymphoma: A case report  
*Xu XL, Zhang RH, Wang YH, Zhou JY*
- 6443** Disseminated infection by *Fusarium solani* in acute lymphocytic leukemia: A case report  
*Yao YF, Feng J, Liu J, Chen CF, Yu B, Hu XP*
- 6450** Primary hepatic neuroendocrine tumor – <sup>18</sup>F-fluorodeoxyglucose positron emission tomography/computed tomography findings: A case report  
*Rao YY, Zhang HJ, Wang XJ, Li MF*
- 6457** Malignant peripheral nerve sheath tumor in an elderly patient with superficial spreading melanoma: A case report  
*Yang CM, Li JM, Wang R, Lu LG*
- 6464** False positive anti-hepatitis A virus immunoglobulin M in autoimmune hepatitis/primary biliary cholangitis overlap syndrome: A case report  
*Yan J, He YS, Song Y, Chen XY, Liu HB, Rao CY*
- 6469** Successful totally laparoscopic right trihepatectomy following conversion therapy for hepatocellular carcinoma: A case report  
*Zhang JJ, Wang ZX, Niu JX, Zhang M, An N, Li PF, Zheng WH*
- 6478** Primary small cell esophageal carcinoma, chemotherapy sequential immunotherapy: A case report  
*Wu YH, Zhang K, Chen HG, Wu WB, Li XJ, Zhang J*
- 6485** Subdural fluid collection rather than meningitis contributes to hydrocephalus after cervical laminoplasty: A case report  
*Huang HH, Cheng ZH, Ding BZ, Zhao J, Zhao CQ*
- 6493** Phlegmonous gastritis developed during chemotherapy for acute lymphocytic leukemia: A case report  
*Saito M, Morioka M, Izumiyama K, Mori A, Ogasawara R, Kondo T, Miyajima T, Yokoyama E, Tanikawa S*
- 6501** Spinal epidural hematoma after spinal manipulation therapy: Report of three cases and a literature review  
*Liu H, Zhang T, Qu T, Yang CW, Li SK*
- 6510** Abdominal hemorrhage after peritoneal dialysis catheter insertion: A rare cause of luteal rupture: A case report  
*Gan LW, Li QC, Yu ZL, Zhang LL, Liu Q, Li Y, Ou ST*
- 6515** Concealed mesenteric ischemia after total knee arthroplasty: A case report  
*Zhang SY, He BJ, Xu HH, Xiao MM, Zhang JJ, Tong PJ, Mao Q*
- 6522** Chylothorax following posterior low lumbar fusion surgery: A case report  
*Huang XM, Luo M, Ran LY, You XH, Wu DW, Huang SS, Gong Q*
- 6531** Non-immune hydrops fetalis: Two case reports  
*Maranto M, Cigna V, Orlandi E, Cucinella G, Lo Verso C, Duca V, Picciotto F*

- 6538** Bystander effect and abscopal effect in recurrent thymic carcinoma treated with carbon-ion radiation therapy: A case report  
*Zhang YS, Zhang YH, Li XJ, Hu TC, Chen WZ, Pan X, Chai HY, Ye YC*
- 6544** Management of an intracranial hypotension patient with diplopia as the primary symptom: A case report  
*Wei TT, Huang H, Chen G, He FF*
- 6552** Spontaneous rupture of adrenal myelolipoma as a cause of acute flank pain: A case report  
*Kim DS, Lee JW, Lee SH*
- 6557** Neonatal necrotizing enterocolitis caused by umbilical arterial catheter-associated abdominal aortic embolism: A case report  
*Huang X, Hu YL, Zhao Y, Chen Q, Li YX*
- 6566** Primary mucosa-associated lymphoid tissue lymphoma in the midbrain: A case report  
*Zhao YR, Hu RH, Wu R, Xu JK*
- 6575** Extensive cutaneous metastasis of recurrent gastric cancer: A case report  
*Chen JW, Zheng LZ, Xu DH, Lin W*

**ABOUT COVER**

Editorial Board Member of *World Journal of Clinical Cases*, Salma Ahi, MD, Assistant Professor, Research Center for Noncommunicable Diseases, Jahrom University of Medical Sciences, Jahrom 193, Iran. salmaahi.61@gmail.com

**AIMS AND SCOPE**

The primary aim of *World Journal of Clinical Cases* (*WJCC*, *World J Clin Cases*) is to provide scholars and readers from various fields of clinical medicine with a platform to publish high-quality clinical research articles and communicate their research findings online.

*WJCC* mainly publishes articles reporting research results and findings obtained in the field of clinical medicine and covering a wide range of topics, including case control studies, retrospective cohort studies, retrospective studies, clinical trials studies, observational studies, prospective studies, randomized controlled trials, randomized clinical trials, systematic reviews, meta-analysis, and case reports.

**INDEXING/ABSTRACTING**

The *WJCC* is now indexed in Science Citation Index Expanded (also known as SciSearch®), Journal Citation Reports/Science Edition, Scopus, PubMed, and PubMed Central. The 2021 Edition of Journal Citation Reports® cites the 2020 impact factor (IF) for *WJCC* as 1.337; IF without journal self cites: 1.301; 5-year IF: 1.742; Journal Citation Indicator: 0.33; Ranking: 119 among 169 journals in medicine, general and internal; and Quartile category: Q3. The *WJCC*'s CiteScore for 2020 is 0.8 and Scopus CiteScore rank 2020: General Medicine is 493/793.

**RESPONSIBLE EDITORS FOR THIS ISSUE**

Production Editor: Yan-Xia Xing; Production Department Director: Yan-Jie Ma; Editorial Office Director: Jin-Lai Wang.

**NAME OF JOURNAL**

*World Journal of Clinical Cases*

**ISSN**

ISSN 2307-8960 (online)

**LAUNCH DATE**

April 16, 2013

**FREQUENCY**

Thrice Monthly

**EDITORS-IN-CHIEF**

Dennis A Bloomfield, Sandro Vento, Bao-Gan Peng

**EDITORIAL BOARD MEMBERS**

<https://www.wjgnet.com/2307-8960/editorialboard.htm>

**PUBLICATION DATE**

August 6, 2021

**COPYRIGHT**

© 2021 Baishideng Publishing Group Inc

**INSTRUCTIONS TO AUTHORS**

<https://www.wjgnet.com/bpg/gerinfo/204>

**GUIDELINES FOR ETHICS DOCUMENTS**

<https://www.wjgnet.com/bpg/GerInfo/287>

**GUIDELINES FOR NON-NATIVE SPEAKERS OF ENGLISH**

<https://www.wjgnet.com/bpg/gerinfo/240>

**PUBLICATION ETHICS**

<https://www.wjgnet.com/bpg/GerInfo/288>

**PUBLICATION MISCONDUCT**

<https://www.wjgnet.com/bpg/gerinfo/208>

**ARTICLE PROCESSING CHARGE**

<https://www.wjgnet.com/bpg/gerinfo/242>

**STEPS FOR SUBMITTING MANUSCRIPTS**

<https://www.wjgnet.com/bpg/GerInfo/239>

**ONLINE SUBMISSION**

<https://www.f6publishing.com>

## Observational Study

# Selection of internal fixation method for femoral intertrochanteric fractures using a finite element method

Jia-Xuan Mu, Shi-Yang Xiang, Qing-Yu Ma, Hai-Lun Gu

**ORCID number:** Jia-Xuan Mu 0000-0003-1233-8386; Shi-Yang Xiang 0000-0002-4917-4357; Qing-Yu Ma 0000-0002-4033-5097; Hai-Lun Gu 0000-0001-5697-9818.

**Author contributions:** Mu JX conceived and coordinated the study, designed, performed, and analyzed the experiments, and wrote the paper; Xiang SY, Ma QY, and Gu HL carried out data collection and analysis and revised the paper; all authors reviewed the results and approved the final version of the manuscript.

**Institutional review board**

**statement:** The study was reviewed and approved by the ethic committee of Shengjing Hospital, China Medical University.

**Informed consent statement:** All study participants, or their legal guardian, provided informed written consent prior to study enrollment.

**Conflict-of-interest statement:**

There are no conflicts of interest to report.

**Data sharing statement:** No additional data are available.

**STROBE statement:** The authors have read the STROBE

Jia-Xuan Mu, Shi-Yang Xiang, Qing-Yu Ma, Hai-Lun Gu, Department of Orthopedics, Shengjing Hospital, China Medical University, Shenyang 117004, Liaoning Province, China

**Corresponding author:** Hai-Lun Gu, PhD, Doctor, Department of Orthopedics, Shengjing Hospital, China Medical University, No. 36 Sanhao Street, Heping District, Shenyang 117004, Liaoning Province, China. [guhailun\\_@163.com](mailto:guhailun_@163.com)

**Abstract****BACKGROUND**

Failure to fix unstable intertrochanteric fractures impairs return to daily activities.

**AIM**

To simulate five different internal fixation methods for unstable proximal femoral fractures.

**METHODS**

A three-dimensional model of the femur was established from sectional computed tomography images, and an internal fixation model was established. Finite element analysis of the femur model was established, and three intertrochanteric fracture models, medial defect, lateral defect, and medial-lateral defects, were simulated. Displacement and stress distribution after fixation with a proximal femoral anti-rotation intramedullary nail (PFNA), integrated dual-screw fixation (ITN), PFNA + wire, PFNA + plate, and PFNA + wire + plate were compared during daily activities.

**RESULTS**

The maximum displacement and stress of PFNA and ITN were 3.51 mm/473 MPa and 2.80 mm/588 MPa for medial defects; 2.55 mm/288 MPa and 2.10 mm/307 MPa for lateral defects; and 3.84 mm/653 MPa and 3.44 mm/641 MPa for medial-lateral defects, respectively. For medial-lateral defects, reconstructing the medial side alone changed the maximum displacement and stress to 2.79 mm/515 MPa; reconstructing the lateral side changed them to 3.72 mm/608 MPa, when both sides were reconstructed, they changed to 2.42 mm/309 MPa.

**CONCLUSION**

For medial defects, intramedullary fixation would allow early low-intensity rehabilitation exercise, and ITN rather than PFNA reduces the risk of varus and cut-out; for lateral wall defects or weakness, intramedullary fixation allows

Statement—checklist of items, and the manuscript was prepared and revised according to the STROBE Statement—checklist of items.

**Open-Access:** This article is an open-access article that was selected by an in-house editor and fully peer-reviewed by external reviewers. It is distributed in accordance with the Creative Commons Attribution NonCommercial (CC BY-NC 4.0) license, which permits others to distribute, remix, adapt, build upon this work non-commercially, and license their derivative works on different terms, provided the original work is properly cited and the use is non-commercial. See: <http://creativecommons.org/licenses/by-nc/4.0/>

**Manuscript source:** Unsolicited manuscript

**Specialty type:** Medicine, research and experimental

**Country/Territory of origin:** China

**Peer-review report's scientific quality classification**

Grade A (Excellent): 0  
 Grade B (Very good): 0  
 Grade C (Good): 0  
 Grade D (Fair): 0  
 Grade E (Poor): 0

**Received:** April 7, 2021

**Peer-review started:** April 7, 2021

**First decision:** April 23, 2021

**Revised:** May 23, 2021

**Accepted:** June 3, 2021

**Article in press:** June 3, 2021

**Published online:** August 6, 2021

**P-Reviewer:** Tribst JPM

**S-Editor:** Fan JR

**L-Editor:** Wang TQ

**P-Editor:** Wang LL



higher-intensity rehabilitation exercise, and ITN reduces the risk of varus. For both medial and lateral defects, intramedullary fixation alone will not allow early functional exercise, but locating lateral or medial reconstruction will. For defects in both the inner and outer sides, if reconstruction cannot be completed, ITN is more stable.

**Key Words:** Hip fractures; Fracture fixation, Intramedullary; Finite element analysis

©The Author(s) 2021. Published by Baishideng Publishing Group Inc. All rights reserved.

**Core Tip:** This study modeled different internal fixation methods for unstable proximal femoral fractures. Finite element analysis of the femur model was established and three intertrochanteric fracture models were simulated. For medial defects, intramedullary fixation would allow early low-intensity rehabilitation exercise, and integrated dual-screw fixation (ITN) rather than proximal femoral anti-rotation intramedullary nail reduces the risk of varus and cut-out; for lateral wall defects or weakness, intramedullary fixation allows higher-intensity rehabilitation exercise, and ITN reduces the risk of varus. For both medial and lateral defects, intramedullary fixation alone will not allow early functional exercise but locating lateral or medial reconstruction will.

**Citation:** Mu JX, Xiang SY, Ma QY, Gu HL. Selection of internal fixation method for femoral intertrochanteric fractures using a finite element method. *World J Clin Cases* 2021; 9(22): 6343-6356

**URL:** <https://www.wjgnet.com/2307-8960/full/v9/i22/6343.htm>

**DOI:** <https://dx.doi.org/10.12998/wjcc.v9.i22.6343>

## INTRODUCTION

An intertrochanteric fracture is a common fracture in the elderly, accounting for about half of the 258000 hip fractures in the United States each year[1]. The prevalence of hip fractures increases significantly as people reach more than 70 years of age[2]. The main goal of treating intertrochanteric fractures is to return to the pre-injury state as soon as possible and achieve early weight-bearing. In the past 40 years, the improvement of implants has achieved consistently good results for stable intertrochanteric fractures, but the treatment failure rate of unstable fractures is still much higher. Unstable intertrochanteric fractures include posterior medial comminutions, lateral wall defects, and reverse oblique fractures[3]. The most common type is the posterior medial comminuted type (AO 31A1.3), followed by a defect of the lateral wall, while reverse oblique fractures are relatively rare[4]. There is a tendency for hip varus and excessive collapse after unstable intertrochanteric fractures, which may lead to postoperative pain, dysfunction, and even implantation failure[5]. This is contrary to the early recovery of the preoperative state that we pursue. Therefore, in-depth research on the biomechanical mechanism of unstable intertrochanteric fractures to achieve fixation allowing early weight-bearing and complete daily activities is required.

In 1949, Evans proposed that reconstruction of the medial cortical continuity can transform unstable fractures into stable fractures. Many anatomical studies found that there is a thickened bone band in the posterior medial side of the femur, which can redistribute the stress to the anterior and lateral sides[6]. Therefore, destruction of the posterior medial side means that the fracture can easily collapse due to axial load, which may cause hip varus. Some studies have shown that reconstruction of the posterior medial cortex can promote fracture healing and reduce postoperative complications[7]. Gotfried[8] first proposed the “lateral wall” concept through retrospective research and pointed out that the lateral wall should be paid attention to in surgery. Im *et al*[9] and Palm *et al*[10] also through retrospective studies, once again confirmed the “lateral wall” concept and pointed out its scope: In the lateral side, the area formed by the plane from the lateral femoral muscle crest to the midpoint of the trochanter. Niu *et al*[11] pointed out that it has an important impact on the efficacy of surgery. The complete lateral wall of the proximal femur can play a good role in supporting the proximal femoral bone. If the lateral wall structure is damaged during

or after surgery, it is lost. The support of the medial bone block will lead to failure of the internal fixation and failure of the operation.

With the introduction of intramedullary fixation, the intramedullary nail system has become a new promising method for the treatment of femoral intertrochanteric fractures. Studies have shown that for unstable intertrochanteric fractures, the application of an intramedullary fixation system can achieve better results[12]. Abram *et al*[13] believe that the three-point stable structure of the proximal femur, that is, the TAD of the head nail, the integrity of the lateral wall where the cephalomedullary nail enter, the integrity of the insertion point of the greater trochanter, and the integrity of the lateral wall is the most important. The biomechanical[14] experiments of Nie *et al*[14] show that the effect of a medial defect alone on the biomechanical stability of the proximal femur is greater than that of lateral wall defect alone. Therefore, it is unclear whether a medial defect or lateral wall defect has a more important effect on stability. As a new type of intramedullary fixation, integrated dual-screw fixation (ITN) has a better effect than traditional gamma nail and anti-rotation blade[15]. This study aimed to find a biomechanical answer.

Clinical studies suggested the biomechanical properties of the proximal femur still need to be fully understood. With the progress of computer science, there has been increasing interest in the application of a finite element method for biomechanical analysis. This study was based on finite element analysis to analyze the biomechanical stability of femoral intertrochanteric fractures involving lateral and medial defects after the application of different internal fixators in order to provide the best set of internal fixation options for femoral intertrochanteric fractures involving lateral and medial defects.

---

## MATERIALS AND METHODS

---

### **Experimental materials**

Experimental specimens were selected from a 30-year-old healthy male volunteer who signed an informed consent form before undergoing scanning for medical images. The subject was 172 cm in height and 70 kg in weight and denied a history of femur trauma. X-ray was used to rule out pathological changes and injuries. All instruments and equipment were in Shengjing Hospital Affiliated with China Medical University.

### **Construction of a three-dimensional model of the normal femur**

With the volunteer in a supine position, the phantom was placed under the examination area and the scanning bed adjusted so that the scanning area was located centrally. Scanning [PhilipsBrilliance128 spiral computed tomography (CT) scanner] was undertaken with the following conditions: 120 kV, 125 mA, slice thickness 1 mm, and spiral axial scanning of the whole bilateral femur from top to bottom. After the original data were interpolated and magnified on a computer (Lenovo), continuous pictures with layer thickness were obtained and recorded in the Digital Imaging and Communications in Medicine (DICOM) format and saved onto a CD. The CT cross-sectional images of the femur in DICOM format were imported into the medical image processing software Mimics 17.0 (Materialise, Leuven, Belgium) for denoising. The ideal boundary threshold of the bone and soft tissue was defined, the soft tissue image around the bone was removed, and the images were selectively segmented according to the anatomical structure. All parts of the femur were aligned to fill the small gaps, make the outer contour of the femur smooth and continuous, and establish a geometric model of the femur (Figure 1). The constructed femur information was saved as a standard tessellation language (STL) format file, and the reverse engineering software Geomagic Studio 2012 (3D Systems, Rock Hill, SC, United States) was used to repair and optimize the STL format file. First, the non-feature blocks and dents on the model surface were removed, and the loose model surface was smoothed to prevent the generation of non-feature high curvature and self-intersecting surfaces. Then, the smooth curved surface was used to fit the triangle surface of the model, and finally, a continuous curved surface model was generated. The femoral cortical bone and cancellous bone were distinguished by the offset function.

### **Design and construction of different fracture models**

For the design of the posterior medial defect, according to the research of Xiong *et al*, we found that the posterior medial defect can reach 39% of the perimeter of the femur at the lesser trochanter level[16]. Combined with the analysis of the shape of the posterior medial fracture block by Gaurav *et al*[17], we designed the size of the medial

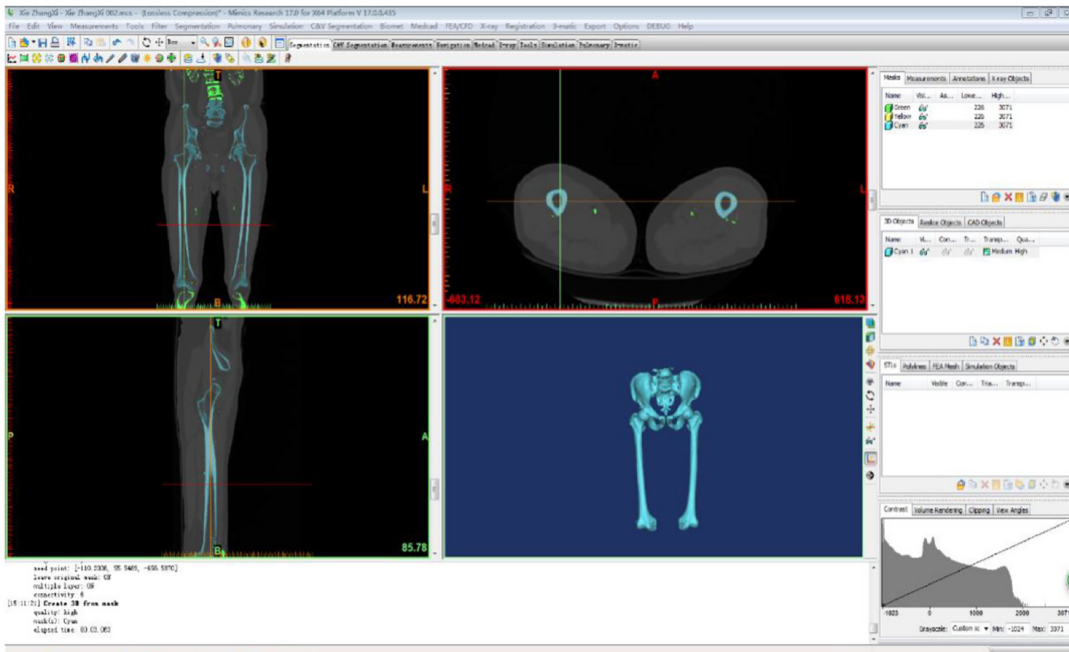


Figure 1 Geometric model of the femur.

injury (model a) as shown in Figure 2A, which is closer to the real medial injury seen in clinic. At the same time, from the mechanical point of view, this size of injury can well simulate the mechanical state of the proximal femur after the medial result is destroyed.

In recent years, the concept of the lateral wall of the femur has been gradually accepted by orthopedic surgeons. The lateral wall has an important influence on the postoperative stability of intertrochanteric fracture. In clinic, complete rupture of the lateral wall is relatively rare, and it is more due to the weakness of the lateral wall caused by the injury, so we designed the lateral wall injury as a bone cortical defect around the main nail (model b) as shown in Figure 2B, which can simulate the more common lateral wall defect in clinic.

By combining the medial defect model with the lateral defect model, the medial and lateral defect model (model c) can be obtained (Figure 2C).

### Design and construction of internal fixation model

A proximal femoral anti-rotation intramedullary nail (PFNA) was selected as a representative and reliable method of intramedullary fixation, as shown in model 1 of Figure 3A. In this experiment, a group of interlocking intramedullary nails were designed for comparison, as shown in model 2 of Figure 3B. A reconstruction model was created according to Kulkarni *et al*[18] to verify its reliability as model 3 (Figure 3C).

It is still controversial whether the lateral wall needs to be reconstructed according to Abram's "three-point stability" theory[13]. Therefore, a lateral wall protection plate combined with PFNA was designed, as model 4 shown in Figure 3D. At the same time, the method of steel wire encircling can also be applied to the reconstruction of the lateral defect.

Without considering the difficulty of the operation, to test whether internal and external construction carried out at the same time would better restore the mechanical stability of the proximal femur, model 3 was designed as shown in Figure 3C, which uses a steel wire to close the internal and external fracture pieces. When also using the outer steel plate to repair the outside, the inner side can also be ligated with the steel wire; model 5 was designed as shown in Figure 3E.

In the anti-rotation intramedullary nail fixation model, the anti-rotation blade of the PFNA was located at the middle and lower 1/3 of the femoral neck. The screw tip was 10 mm away from the femoral boundary, and the lateral view was in the center of the femoral neck. In order to ensure the comparability of PFNA and ITN, the axes of the cephalospinal nails of the two were kept consistent. The lateral greater tuberosity protective plate surrounded the tail of the cephalad nail, and its midline was consistent with the lateral long axis of the femur. Using the candy paper wrapping

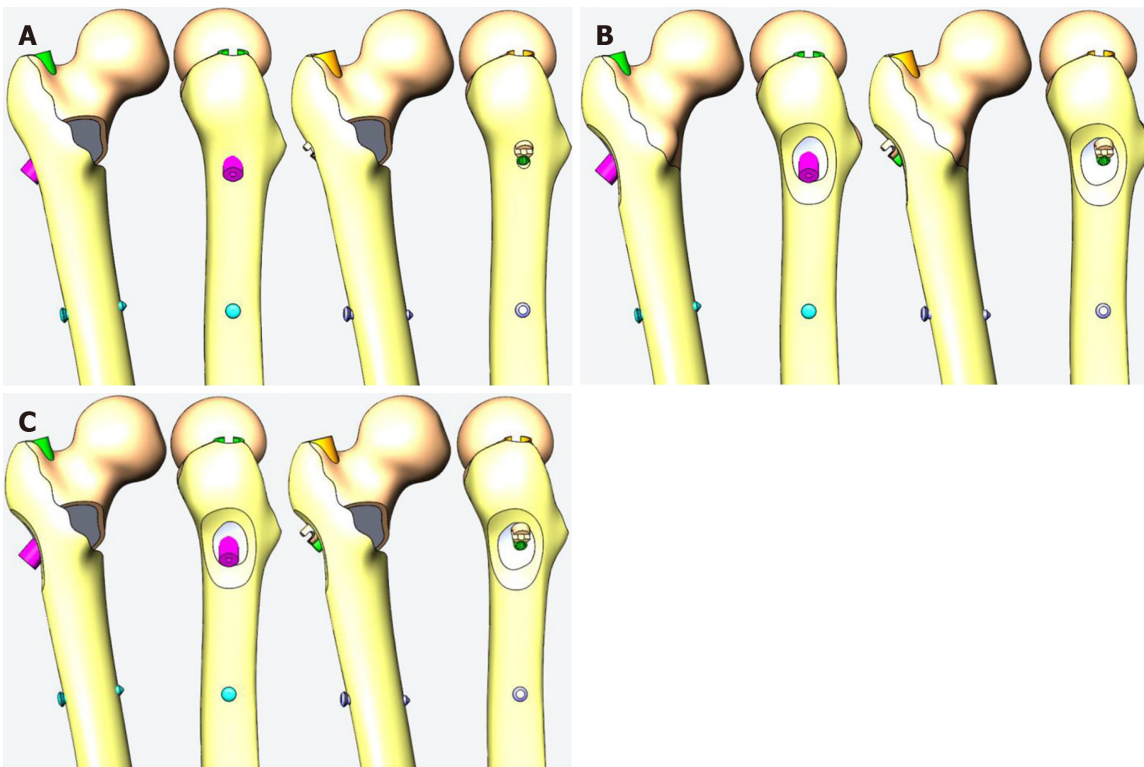


**Figure 2** Medial injury models in the 3D-model. A: Medial defect model; B: Lateral defect model; C: Lateral and medial defect model.

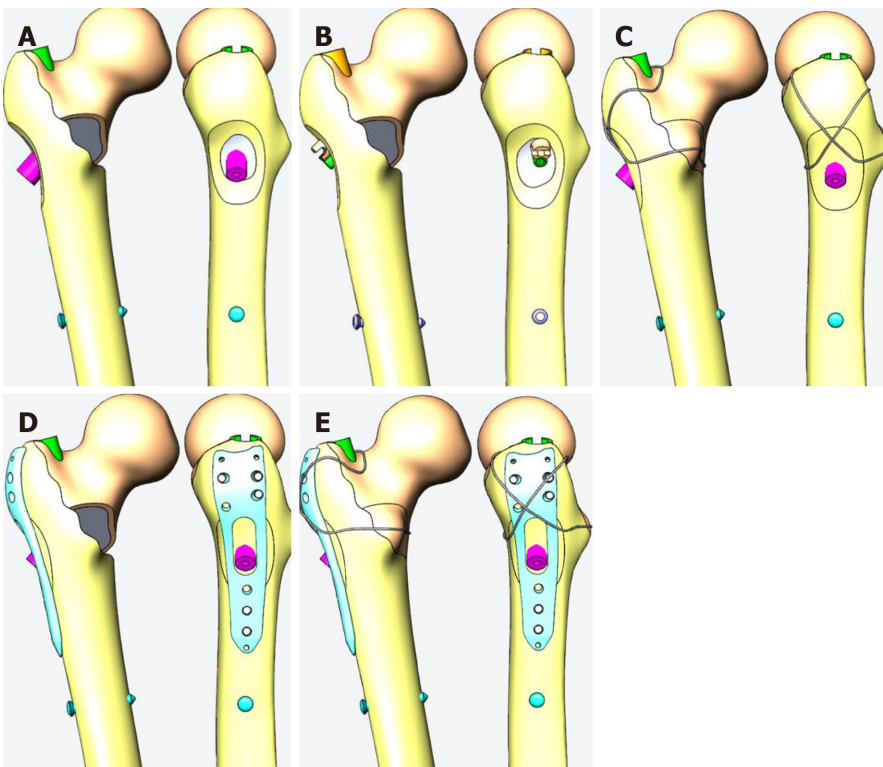


**Figure 3** Fixation models in the 3D model. A: Proximal femoral anti-rotation intramedullary nail (PFNA) representing intramedullary fixation model 1; B: Interlocking intramedullary nails model 2; C: PFNA and steel wire model 3; D: PFNA and interlocking plate model 4; E: PFNA with wire and plate model 5.

method, the upper edge of the steel wire group was along the upper part of the femoral neck, and the lower part was along the lower part of the lesser trochanter to pressurize the lesser trochanter. The two upper and lower branches crossed over the outer side of the tail of the cephalad nail to compress the greater trochanter bone. In

the steel wire and steel plate combined group, the position of the steel plate was the same as the position of the steel plate group alone, the upper and lower positions of the steel wire relative to the femoral neck were the same as mentioned above, and the steel wires crossed on the outside of the steel plate.

For the meshing process, the intramedullary nails, proximal spiral blades, and distal transverse locking nails were edited as a standard tetrahedral mesh with a size of 2 mm. The femoral cortical bone and femoral cancellous bone were divided into standard tetrahedral meshes with a size of 3.5 mm. The numbers of elements and nodes of the models are shown in [Supplementary Table 1](#). The contact properties of the bone-metal contact were set with a friction coefficient of 0.2, except for ITN tension nails and compression nails in which some threads were set to bind. The threaded area was the set binding, and the non-threaded area was the contact attribute with a friction coefficient of 0.2[19,20].

### **Design and construction of three-dimensional finite element models of femoral trochanter fracture**

The internal fixation model was constructed with Solidworks software (French Dassault), and the internal fixation system was based on PFNA intramedullary nail and combined pressurized intramedullary nail produced by Double Technology Co., Ltd. The solid model of the femur generated by GeomagicStudio was imported into the design software Solidworks in IGES format to simulate trochanter fractures with medial defect, lateral defect, and both lateral and medial defects, and combined with the established internal fixation models to establish three-dimensional finite element models of femoral trochanter fractures (Abaques 6.14) with different internal fixation methods. The statistics of the three assembly elements and the total numbers of nodes are shown in [Table 1](#).

### **Boundary and loading**

In the current study, the maximum stress and maximum displacement were obtained with Abaqus 6.14 (Dassault, France). Bergmann *et al*[21] showed that when standing still, standing on one leg, and going up and downstairs, the loading stress during normal walking was 100%-140% body weight (BW), 232%-369% BW, 227%-316% BW, and 211%-285% BW, respectively. The average range of peak load in daily life is 50%-350% BW. In the current research, to simplify the calculations, 100% BW was used when standing normally, 200% BW for slow walking, 250% BW for fast walking, and 300% BW for walking downstairs. Using this information with the three-dimensional model, the following four representative exercise modes in daily life were designed: Standing model A: This model simulated the hip load of a 70 kg adult male standing normally, the loading stress was 700 N vertically downward, and the hip adduction was 15°; slow walking model B: This model simulated the maximum hip load during slow walking during rehabilitation exercise after surgery. The rehabilitation training of patients was measured 3 d after the operation, and their step length interval was 46-58 cm, which was slightly smaller than that of healthy elderly[22]. In order to simplify the calculation, 50 cm was set in the slow walk model to get the hip load mode, the loading stress was 1400 N vertically downward, hip adduction was 10°, flexion 17°, and external rotation 15°; normal walking model C: This model simulated the maximum load of the hip during walking of the healthy elderly. The step size was set to 60 cm. In the normal walking state, the impulse on the hip is greater, the range of movement is greater, and the corresponding loading stress is greater. Therefore, the hip load mode was set to 1750 N vertically downward, hip adduction was 10°, flexion 20°, and external rotation 15°; and stair descent model D: This model simulated the maximum load of the hip when the healthy elderly place one side of the foot in contact with the ground when descending down a step, which is usually the maximum load on the hip in daily life[21]. However, patients with femoral intertrochanteric fractures rarely complete this action after a recent operation. The impulse on the hip is very large, but the range of hip joint movement is small. The load was set to 2100 N vertically downward, hip adduction was 10°, flexion 10°, and external rotation 15°.

After setting the loading mode, it was assumed that the fracture surface was completely broken and in the contact state, and the friction coefficient was 0.2[23]. The femur bears many loads, including muscle force, joint force, and dynamic impact force. It is complicated to simulate this load with finite element analysis. In view of many uncertainties in the finite element simulation of muscle loading, including the number and direction of selected loads, it is more difficult to accurately simulate the dynamic load[24]. This experiment simplified the model and analyzed the compression load of the model. The load of the femur of the human body under four loading

**Table 1** Material properties of the femur and internal fixation model[28,29]

Material	Elastic modulus (Mpa)	Poisson ratio
Cortical bone	16800	0.29
Cancellous bone	260	0.2
Internal fixation	110000	0.3

modes was simulated, with different loads on the outer surface of the contact area between the femoral head and the acetabulum along the direction of the force line. Schneider *et al*[25], after measuring the load of the model of femoral shaft fracture fixed with an intramedullary nail, found that the femur was subjected to 2-5 N·m torque when the human body was walking with weight. Duda *et al*[26] reported that the maximum torsional load on the femur is about 0.01 body weight per meter after the femoral shaft fracture is fixed with an intramedullary nail, so the maximum torque on the femur is 7 N·m according to the BW of 700 N. Therefore, in the compression + torsion analysis, the boundary load condition was distally fixed. Different vertical loads and 7 N·m external rotation torque were applied at the proximal end of the femur, regardless of the specific role of each muscle group.

The established femoral cortical bone model, femoral cancellous bone model, and internal fixation three-dimensional finite element model were imported into Solidworks for assembly, and pre-load experiments were carried out according to the previous references[15,17]. This calculated, according to the axial load and boundary conditions, the obtained femoral contact pressure (7.58 Mpa), which is similar to the pressure value of 5-10 Mpa in the literature, so the model in this study can be judged to be reliable and effective.

### Experimental grouping

The three types of models were then combined to alter fracture types, internal fixation types, and loading modes as shown in Table 2 to compare the maximum stress and displacement of each combination. Since the convergence difference of the results of the finite element analysis in this study was less than 5%, it could be considered that there was a unique solution, and statistical analysis was not required.

## RESULTS

The maximum stress and maximum displacement of the different types of defects under each loading model are summarized in Table 3 and are shown in detail in Supplementary Figures 1-9. In each model of defect and fixation, as expected, the maximum values were found with the stair descent model D.

For PFNA fixation of a medial defect, the maximum displacement and stress were 3.51 mm/473 MPa (Table 3 and Supplementary Figure 1). For a lateral defect, the corresponding values were 2.55 mm/288 MPa (Supplementary Figure 2), and for both lateral and medial defects, they were 3.84 mm/653 MPa (Figure 4).

For ITN fixation of a medial defect, the maximum displacement and stress were 2.80 mm/588 MPa (Table 3 and Supplementary Figure 3). For a lateral defect, the values were 2.10 mm/307 MPa (Supplementary Figure 4), and for lateral and medial defects together, they were 3.44 mm/641 MPa (Figure 5).

We tested whether internal and external construction carried out at the same time would better restore mechanical stability of the proximal femur with both lateral and medial defects (model c). In the case of reconstructing the lateral side using PFNA and a plate, the values changed to 3.72 mm/608 MPa (Table 3 and Supplementary Figure 5). In the case of reconstructing the medial side alone using PFNA and wire, the maximum values changed to 2.79 mm/515 MPa (Table 3 and Supplementary Figure 6). When both the medial and lateral sides were reconstructed using PFNA with wire and a plate, the numerical value changed to 2.42 mm/309 MPa (Table 3 and Figure 6).

## DISCUSSION

This study analyzed the achievable effects of different internal fixation methods for unstable proximal femoral fractures from the perspective of biomechanics to provide a

**Table 2 Grouping according to different models**

	Normal standing A			Slow walking B			Fast walking C			Stair descent D		
	Medial defect a	Lateral defect b	Lateral and medial defect c	Medial defect a	Lateral defect b	Lateral and medial defect c	Medial defect a	Lateral defect b	Lateral and medial defect c	Medial defect a	Lateral defect b	Lateral and medial defect c
PFNA 1	1Aa	1Ab	1Ac	1Ba	1Bb	1Bc	1Ca	1Cb	1Cc	1Da	1Db	1Dc
ITN 2	2Aa	2Ab	2Ac	2Ba	2Bb	2Bc	2Ca	2Cb	2Cc	2Da	2Db	2Dc
PFNA + steel wire 3	3Aa	3Ab	3Ac	3Ba	3Bb	3Bc	3Ca	3Cb	3Cc	3Da	3Db	3Dc
PFNA + plate 4		4Ab	4Ac		4Bb	4Bc		4Cb	4Cc		4Db	4Dc
PFNA + steelwire + plate 5		5Ab	5Ac		5Bb	5Bc		5Cb	5Cc		5Db	5Dc

PFNA: Proximal femoral anti-rotation intramedullary nail; ITN: Integrated dual-screw fixation.

**Table 3 Comparison of the maximum stress and maximum displacement among different fixation methods, different stress modes, and different fracture types**

	Normal standing A			Slow walking B			Fast walking C			Stair descent D		
	a	b	c	a	b	c	a	b	c	a	b	c
Maximum stress at the main nail (MPa)												
1	176	92	239	334	183	456	404	235	556	473	288	653
2	203	102	229	402	204	445	496	256	546	588	307	641
3	121	84.8	141	318	173	392	383	219	438	425	265	515
4		89	213		178	416		228	515		278	608
5		67	107		134	205		167	253		203	309
Maximum displacement of proximal femur (mm)												
1	1.22	0.85	1.35	2.39	1.70	2.61	2.95	2.12	3.23	3.51	2.55	3.84
2	0.95	0.69	1.19	1.89	1.39	2.33	2.35	1.74	2.89	2.80	2.10	3.44
3	0.85	0.70	0.93	1.64	1.40	1.82	2.04	1.75	2.29	2.44	2.09	2.79
4		0.84	1.31		1.66	2.52		2.08	3.12		2.49	3.72
5		0.75	0.82		1.49	1.62		1.87	2.02		2.24	2.42

a: Medial defect; b: Lateral defect; c: Lateral and medial defect; 1: PFNA; 2: ITN; 3: PFNA + wire 3; 4: PFNA + plate; 5: PFNA + wire + plate; PFNA: Proximal femoral anti-rotation intramedullary nail; ITN: Integrated dual-screw fixation.

reference for clinical decision-making. The results showed that the maximum displacement and stress of PFNA and ITN were 3.51 mm/473 MPa and 2.80 mm/588 MPa for medial defects; 2.55 mm/288 MPa and 2.10 mm/307 MPa for lateral defects; and 3.84 mm/653 MPa and 3.44 mm/641 MPa for medial-lateral defects, respectively. For medial-lateral defects, reconstructing the medial side alone changed maximum displacement and stress to 2.79 mm/515 MPa; reconstructing the lateral side changed them to 3.72 mm/608 MPa; and when both sides were reconstructed, they changed to 2.42 mm/309 MPa. Therefore, intramedullary fixation would allow early low-intensity rehabilitation exercise for medial defects, while ITN rather than PFNA reduces the risk of varus and cut-out. For lateral wall defects or weakness, intramedullary fixation allows higher-intensity rehabilitation exercise, and ITN reduces the risk of varus. For both medial and lateral defects, intramedullary fixation alone will not allow early functional exercise.

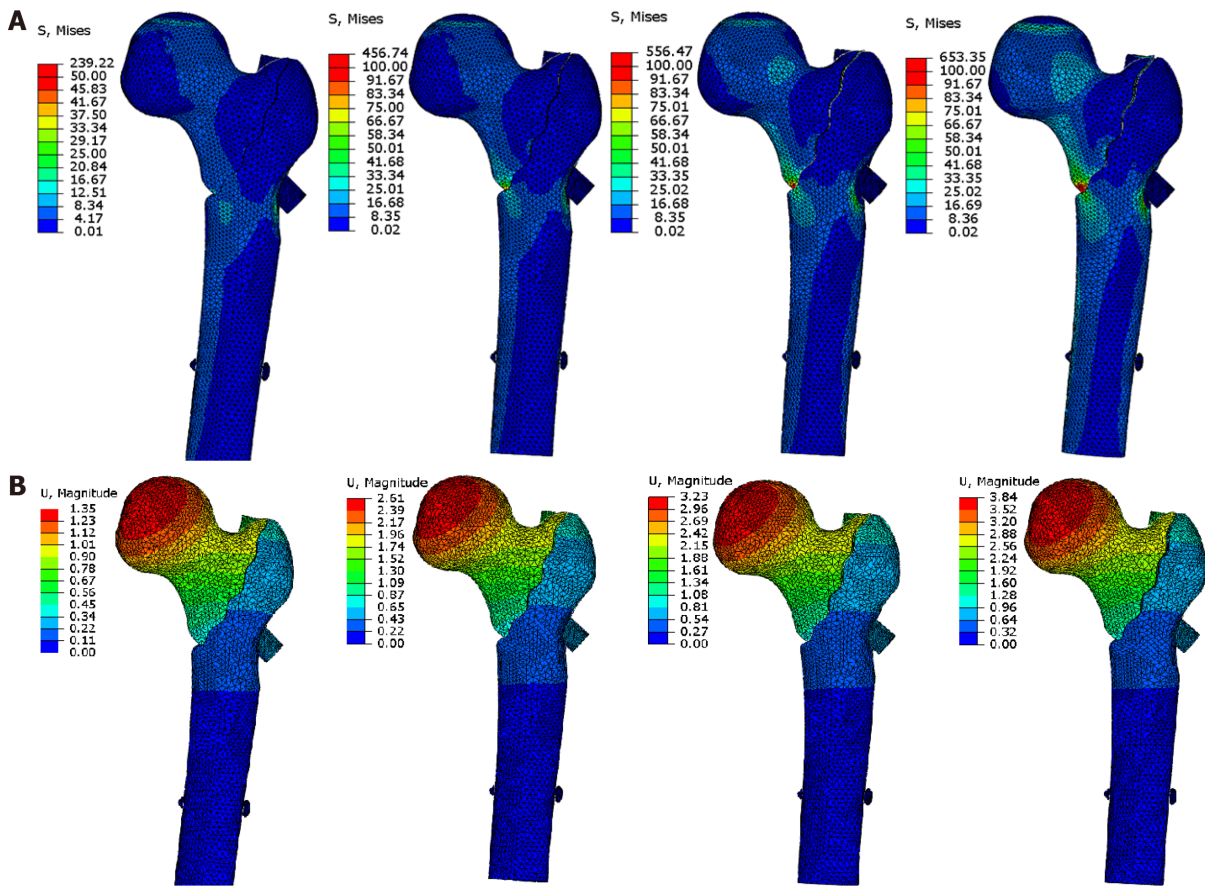


**Figure 4** Stress distribution and displacement distribution under different loading modes when lateral and medial defects were fixed with proximal femoral anti-rotation intramedullary nail. A: Von Mises stress distribution map when lateral and medial defects were fixed with proximal femoral anti-rotation intramedullary nail (PFNA); B: Displacement distribution when lateral and medial defects were fixed with PFNA.

As the stress model changes, the maximum displacement in the model gradually increases. In the displacement distribution diagrams under various models, it can be seen that the maximum displacement is always concentrated at the proximal end of the fracture, which results in varus displacement. This phenomenon is consistent with the same type of simulation carried out by previous researchers[14] and is also consistent with our clinical experience. In different types of internal fixation methods and stress loading modes, the maximum displacement caused by the inner defect model is greater than that of the outer defect model. This expected result is consistent with the physiological structure characteristics of the proximal femur and is also consistent with previous experimental results. When lateral and medial defects are combined, this will greatly increase the degree of varus at the proximal end of the fracture. Since a finite element study cannot simulate the failure load, a relatively objective index is needed in this discussion to analyze the stress magnitude of each point in the model. After consulting the relevant literature, the fatigue limit of titanium alloys at room temperature could be used as a reference index. The fatigue limit refers to the maximum stress value after an infinite number of stress cycles without failure, which is determined by the fatigue test. Generally, the fatigue limit of medical titanium alloys at room temperature is 438 Mpa[27].

In the medial defect model, if medial reconstruction is not performed, although the maximum stress on the ITN main nail is higher than the PFNA, the maximum displacement can be effectively controlled. In the loading models of normal standing and slow walking, the maximum stress of PFNA and ITN did not exceed the fatigue limit, and the stress was within the acceptable range of the internal fixation. The application of ITN can better control the displacement, that is, reduce inversion. Combined with the larger cross-sectional area of the ITN head spinal nail in the sagittal section of the femoral neck, less displacement will also reduce the risk of cut-out. When simulating the walking state and the gait of the healthy elderly, the maximum stress on the main nail exceeds the fatigue limit, and there is a risk of the main nail breaking. If steel wire is used to reconstruct the inner side, the stress distribution diagram shows that the maximum stress is on the steel wire instead of the main

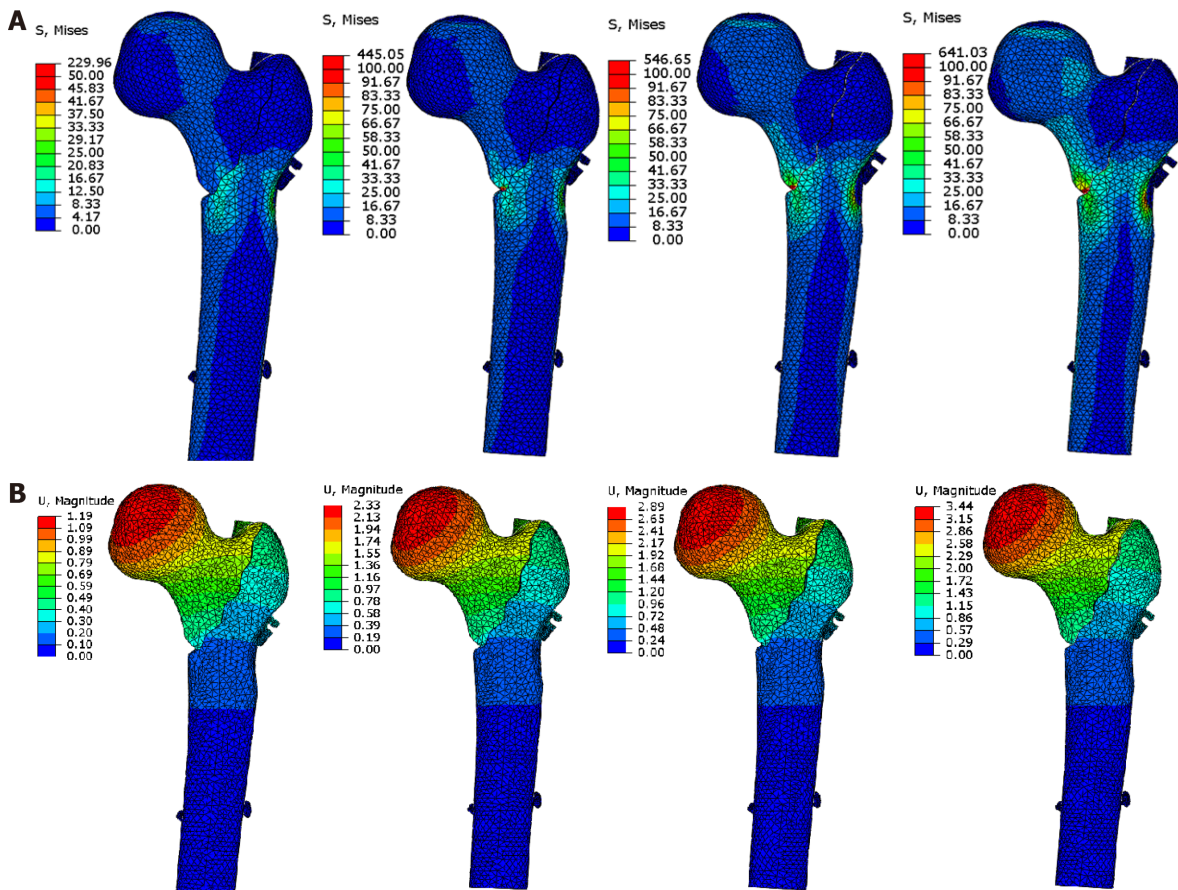


**Figure 5** Stress distribution and displacement distribution under different loading modes when lateral and medial defects were fixed with integrated dual-screw fixation. A: Von Mises stress distribution map when lateral and medial defects were fixed with Integrated dual-screw fixation (ITN); B: Displacement distribution when lateral and medial defects were fixed with ITN.

nail. During the standing model, the stress on the steel wire is smaller. Once the load stress increases, this will inevitably lead to the fracture of the steel wire. Therefore, if it is necessary to reconstruct the inside during the operation, it is recommended to use an internal fixation that can withstand greater tension, such as a titanium cable. However, it should also be noted that compared to the use of a separate intramedullary system for fixation, reconstructing a medial defect with wire can effectively reduce displacement.

In the lateral defect model, without lateral reconstruction, ITN has better control over displacement than PFNA. When simulating walking and walking downstairs, the maximum stress on the main nail does not exceed the fatigue limit. Therefore, for a simple lateral defect, intramedullary fixation can also bear early weight even if the lateral wall is not reconstructed. When reconstructing the lateral defect, reconstruction of the lateral wall with steel wire provided the best displacement control. The two methods of reconstructing the lateral wall can reduce the stress concentration, the maximum stress in the main nail, and the maximum displacement compared with the intramedullary nail alone. Compared with the two reconstruction methods, the displacement and stress control of the external reconstruction using steel plate is worse than that of external reconstruction using steel wire. For a lateral wall defect, using a steel plate and steel wire for reconstruction at the same time is not as good as using steel wire alone. This demonstrates that the effect of the two reconstruction methods is not a simple superposition effect, and even steel plate reconstruction may hinder the effect of steel wire reconstruction. However, it is worth noting that rebuilding the outer side with steel wire will cause a large amount of stress on the steel wire, thus causing the wire to break. If the fracture has not healed, the reconstruction will fail when steel wire breaks, but steel plate reconstruction does not have this problem. At the same time, because wire reconstruction surgical planning is more difficult and requires a longer operation, reconstruction with a steel plate alone might be recommended if the lateral wall needs to be reconstructed.

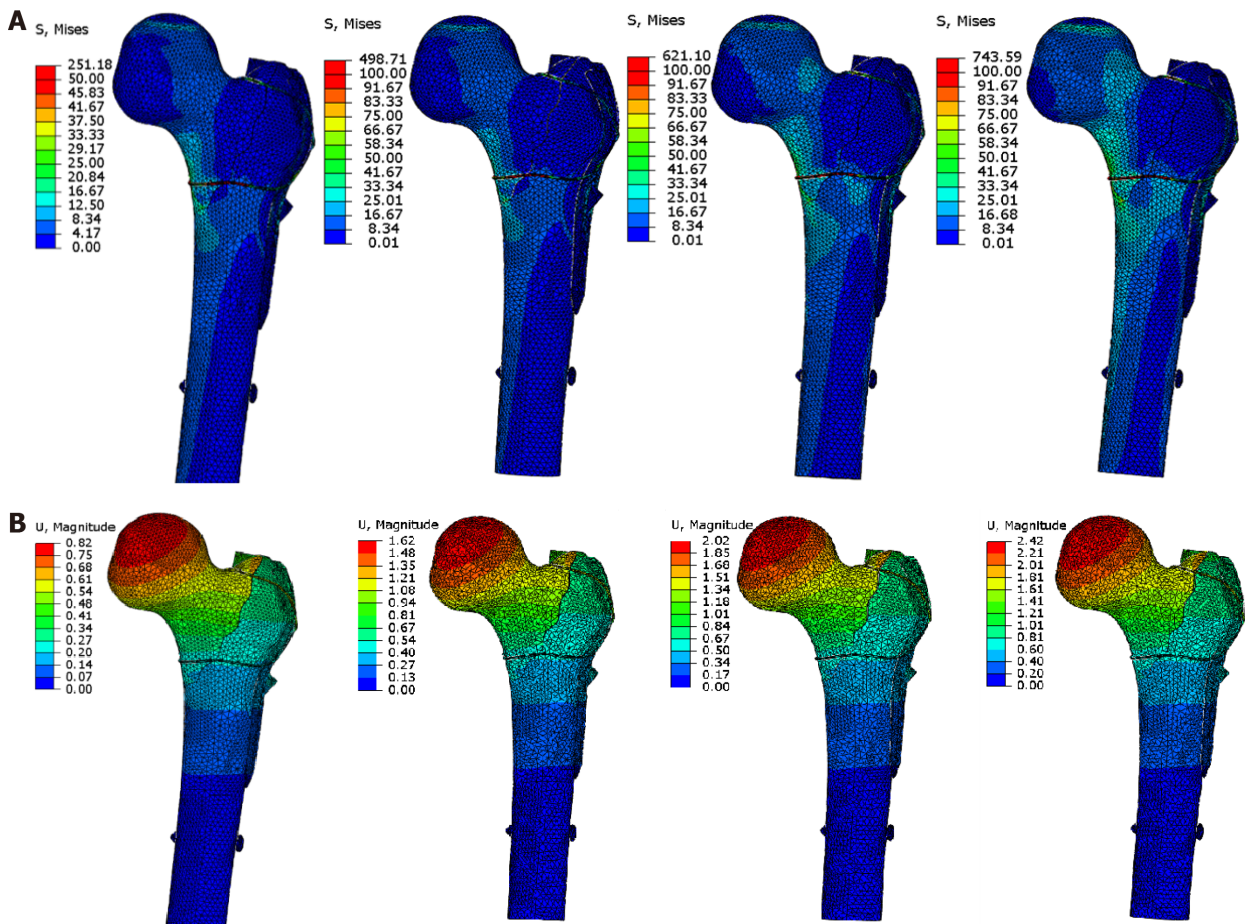


**Figure 6** Stress distribution and displacement distribution under different loading modes when lateral and medial defects were fixed with proximal femoral anti-rotation intramedullary nail steel wire and lateral wall protection plate. A: Von Mises stress distribution map when lateral and medial defects were fixed with proximal femoral anti-rotation intramedullary nail (PFNA), steel wire, and lateral wall protection plate; B: Displacement distribution when lateral and medial defects were fixed with PFNA, steel wire, and lateral wall protection plate.

For both inside and outside defects, much stress will be concentrated on the main nail. In our slow walking model, the maximum stress of the PFNA and ITN groups can reach 456 MPa and 445 MPa, exceeding the fatigue limit of titanium. This means that even with milder rehabilitation when the fracture has not healed completely, there is a risk of fracture of the internal fixation under repeated stress stimulation. Therefore, intramedullary fixation alone allows low-intensity rehabilitation exercises such as early standing. However, the healing of the patient’s fracture must be evaluated before walking; otherwise, it may fracture the internal fixation. Once the bone is healed, these two maximum values should not be a problem since the nail is supported by the bone and *vice versa*. When reconstructing the internal and external defects, this study designed two schemes. One used steel wire to circumscribe the medial bone block while simultaneously reconstructing the lateral defect. The other used a lateral steel plate to reconstruct the lateral defect and cerclage of the medial bone block with steel wire. Any reconstruction program has better control of displacement and stress than using an intramedullary nail alone. The best control on stress and displacement was to apply an outer steel plate and inner steel wire circling group at the same time. The steel plate + steel wire group was more effective than using steel wires to reconstruct the medial and lateral sides. This is because, in the medial defect, the femoral head has a serious tendency to varus. After the intramedullary nail is applied, the varus stress is transmitted to the main nail and the lateral wall through the medullary nail. At this time, there will be axial tension on the outer sidewall. If a steel plate is used for reconstruction, it will resist this tension, but steel wire cannot, resulting in increased proximal displacement. However, related to the previous discussion, when reconstruction is performed on both the inner and outer sides, steel wire plays a major role in the reconstruction of the inner defect. At the same time, during slow walking, the maximum stress of the inner and outer reconstruction groups does not exceed the fatigue strength and is theoretically safe. Therefore, when both the inner and outer

sides are defective, both sides should be reconstructed; the outer side is reconstructed with a steel plate and the inner side with a titanium cable with stronger tensile strength. This allows the patient to perform early low-intensity rehabilitation exercises. Because it is difficult to reconstruct the medial side, it is still recommended to use a steel plate for lateral reconstruction when the medial reconstruction cannot be completed.

In summary, for a posteromedial defect, intramedullary fixation can meet the needs of early low-intensity rehabilitation exercise, and application of ITN compared with PFNA can reduce the risk of varus and cut-out. For a lateral wall defect or weakness, intramedullary fixation can meet the needs of higher-intensity rehabilitation exercise and even a return to the preoperative state. Application of ITN can also reduce the risk of varus. For both lateral and medial defects, fixation with an intramedullary system alone cannot meet the requirements of early functional exercise, but they can be met by choosing a site for lateral or medial reconstruction. However, the preoperative functional state cannot be restored in a short period of time. When there are defects in both the inner and outer sides, if reconstruction of the inside and outside cannot be completed due to technical conditions, the stability of the ITN system is better. In the case of a medial defect, compared with the application of intramedullary system fixation alone, the method of medial reconstruction with steel wire can effectively reduce the displacement. If the lateral wall needs to be reconstructed during the operation, we recommend the use of plate reconstruction alone. In the case of both internal and external defects, we recommend that both the medial and lateral sides be reconstructed; the outer side should be fixed with a steel plate, and the inner side should be fixed with titanium cable with strong tensile strength so that patients can carry out early low-intensity rehabilitation exercises. As medial reconstruction is difficult, when it cannot be completed, lateral reconstruction with a steel plate is still recommended.

A strength of this study is that once the base model and fixation models are designed, it is easy to import the CT images from a given patient and use them to simulate the various fixations. This would allow treatment individualization. This study has some limitations. Human joints are complex in structure with many tissues, including ligaments, cartilage, muscles, and tendons. Mechanical experiments and basic research cannot accurately equate to the variety of tissues involved. The application of bone finite element analysis is mostly based on an assumption of isotropic, homogeneous, and continuous linear elastomers. Because this paper discusses the static stress distribution after plant fixation under various static loads, only bone and internal fixation were considered in the model, regardless of the friction between joints, while cartilage was ignored. Muscle and tendon stresses were simplified. The greatest difficulty in the simulation of a physiological and anatomical model lies in the determination of the material characteristics of various biological tissues because the material properties of biological tissues often depend on certain load conditions, that is, under different physiological loads, the material properties of the same tissue are different. It is generally believed that both cortical bone and cancellous bone can be considered to have linear elastic properties under quasi-static load, and valuable results can be obtained by using linear elastic material to simulate bone under quasi-static load. Therefore, the model assumes that the femoral bone is an isotropic and homogeneous linear elastic material. This study referred to data from previous scholars[28,29]. The models in this study are all ideal in theory, and a large number of factors are simplified, which cannot be completely equated with the situation in the real human body. In the future, we will continue to improve biomechanical analysis and cohort studies of related surgical schemes.

---

## CONCLUSION

---

For medial defects, intramedullary fixation would allow early low-intensity rehabilitation exercise, and ITN rather than PFNA reduces the risk of varus and cut-out; for lateral wall defects or weakness, intramedullary fixation allows higher-intensity rehabilitation exercise, and ITN reduces the risk of varus. For both medial and lateral defects, intramedullary fixation alone will not allow early functional exercise, but locating lateral or medial reconstruction will. For defects in both the inner and outer sides, if reconstruction cannot be completed, ITN is more stable.

## ARTICLE HIGHLIGHTS

### Research background

Failure to fix unstable intertrochanteric fractures impairs return to daily activities.

### Research motivation

To evaluate whether postoperative rehabilitation can be completed with or without medial and lateral support after intramedullary fixation of intertrochanteric fracture.

### Research objectives

To analyze the stress and displacement distribution of unstable intertrochanteric fracture under different stress modes in postoperative rehabilitation.

### Research methods

This study modeled five different internal fixation methods for unstable proximal femoral fractures. The finite element method was used to simulate the stress loading situation under the postoperative activity to a certain extent.

### Research results

The maximum displacement and stress of proximal femoral anti-rotation intramedullary nail and integrated dual-screw fixation (ITN) were 3.51 mm/473 MPa and 2.80 mm/588 MPa for medial defects; 2.55 mm/288 MPa and 2.10 mm/307 MPa for lateral defects; and 3.84 mm/653 MPa and 3.44 mm/641 MPa for medial-lateral defects, respectively. For medial-lateral defects, reconstructing the medial side alone changed maximum displacement and stress to 2.79 mm/515 MPa; reconstructing the lateral side changed them to 3.72 mm/608 MPa; and when both sides were reconstructed, they changed to 2.42 mm/309 MPa.

### Research conclusions

When the inner and outer sides are damaged at the same time, one place should be selected for reconstruction (outer or inner side), and low-intensity rehabilitation exercises can be carried out. When the inner and outer sides are damaged at the same time, if the reconstruction cannot be completed, the stability of the ITN system is better.

### Research perspectives

To develop an effective treatment plan for medial and lateral defects.

## REFERENCES

- 1 **Kim SH**, Meehan JP, Blumenfeld T, Szabo RM. Hip fractures in the United States: 2008 nationwide emergency department sample. *Arthritis Care Res (Hoboken)* 2012; **64**: 751-757 [PMID: [22190474](#) DOI: [10.1002/acr.21580](#)]
- 2 **Ren Y**, Hu J, Lu B, Zhou W, Tan B. Prevalence and risk factors of hip fracture in a middle-aged and older Chinese population. *Bone* 2019; **122**: 143-149 [PMID: [30797059](#) DOI: [10.1016/j.bone.2019.02.020](#)]
- 3 **Tawari AA**, Kempegowda H, Suk M, Horwitz DS. What makes an intertrochanteric fracture unstable in 2015? *J Orthop Trauma* 2015; **29** Suppl 4: S4-S9 [PMID: [25756825](#) DOI: [10.1097/BOT.0000000000000284](#)]
- 4 **Selim AAHA**, Beder FK, Algeaidy IT, Farhat AS, Diab NM, Barakat AS. Management of unstable pertrochanteric fractures, evaluation of forgotten treatment options. *SICOT J* 2020; **6**: 21 [PMID: [32579105](#) DOI: [10.1051/sicotj/2020020](#)]
- 5 **Kregor PJ**, Obremesky WT, Kreder HJ, Swiontkowski MF. Unstable pertrochanteric femoral fractures. *J Orthop Trauma* 2014; **28** Suppl 8: S25-S28 [PMID: [25046412](#) DOI: [10.1097/BOT.0000000000000187](#)]
- 6 **Zhang Q**, Chen W, Liu HJ, Li ZY, Song ZH, Pan JS, Zhang YZ. The role of the calcar femorale in stress distribution in the proximal femur. *Orthop Surg* 2009; **1**: 311-316 [PMID: [22009881](#) DOI: [10.1111/j.1757-7861.2009.00053.x](#)]
- 7 **Wu HF**, Chang CH, Wang GJ, Lai KA, Chen CH. Biomechanical investigation of dynamic hip screw and wire fixation on an unstable intertrochanteric fracture. *Biomed Eng Online* 2019; **18**: 49 [PMID: [31018860](#) DOI: [10.1186/s12938-019-0663-0](#)]
- 8 **Gotfried Y**. The lateral trochanteric wall: a key element in the reconstruction of unstable pertrochanteric hip fractures. *Clin Orthop Relat Res* 2004; **82**: 82-86 [PMID: [15292791](#)]
- 9 **Im GI**, Shin YW, Song YJ. Potentially unstable intertrochanteric fractures. *J Orthop Trauma* 2005;

- 19: 5-9 [PMID: [15668577](#) DOI: [10.1097/00005131-200501000-00002](#)]
- 10 **Palm H**, Jacobsen S, Sonne-Holm S, Gebuhr P; Hip Fracture Study Group. Integrity of the lateral femoral wall in intertrochanteric hip fractures: an important predictor of a reoperation. *J Bone Joint Surg Am* 2007; **89**: 470-475 [PMID: [17332094](#) DOI: [10.2106/jbjs.f.00679](#)]
  - 11 **Niu E**, Yang A, Harris AH, Bishop J. Which Fixation Device is Preferred for Surgical Treatment of Intertrochanteric Hip Fractures in the United States? *Clin Orthop Relat Res* 2015; **473**: 3647-3655 [PMID: [26208608](#) DOI: [10.1007/s11999-015-4469-5](#)]
  - 12 **Nherera L**, Trueman P, Horner A, Watson T, Johnstone AJ. Comparison of a twin interlocking derotation and compression screw cephalomedullary nail (InterTAN) with a single screw derotation cephalomedullary nail (proximal femoral nail antirotation): a systematic review and meta-analysis for intertrochanteric fractures. *J Orthop Surg Res* 2018; **13**: 46 [PMID: [29499715](#) DOI: [10.1186/s13018-018-0749-6](#)]
  - 13 **Abram SG**, Pollard TC, Andrade AJ. Inadequate 'three-point' proximal fixation predicts failure of the Gamma nail. *Bone Joint J* 2013; **95-B**: 825-830 [PMID: [23723280](#) DOI: [10.1302/0301-620X.95B6.31018](#)]
  - 14 **Nie B**, Chen X, Li J, Wu D, Liu Q. The medial femoral wall can play a more important role in unstable intertrochanteric fractures compared with lateral femoral wall: a biomechanical study. *J Orthop Surg Res* 2017; **12**: 197 [PMID: [29282138](#) DOI: [10.1186/s13018-017-0673-1](#)]
  - 15 **Santoni BG**, Diaz MA, Stoops TK, Lannon S, Ali A, Sanders RW. Biomechanical Investigation of an Integrated 2-Screw Cephalomedullary Nail Versus a Sliding Hip Screw in Unstable Intertrochanteric Fractures. *J Orthop Trauma* 2019; **33**: 82-87 [PMID: [30562248](#) DOI: [10.1097/BOT.0000000000001351](#)]
  - 16 **Xiong WF**, Zhang YQ, Chang SM, Hu SJ, Du SC. Lesser Trochanteric Fragments in Unstable Pertrochanteric Hip Fractures: A Morphological Study Using Three-Dimensional Computed Tomography (3-D CT) Reconstruction. *Med Sci Monit* 2019; **25**: 2049-2057 [PMID: [30889172](#) DOI: [10.12659/MSM.913593](#)]
  - 17 **Sharma G**, Gn KK, Khatri K, Singh R, Gamanagatti S, Sharma V. Morphology of the posteromedial fragment in pertrochanteric fractures: A three-dimensional computed tomography analysis. *Injury* 2017; **48**: 419-431 [PMID: [27903406](#) DOI: [10.1016/j.injury.2016.11.010](#)]
  - 18 **Kulkarni SG**, Babhulkar SS, Kulkarni SM, Kulkarni GS, Kulkarni MS, Patil R. Augmentation of intramedullary nailing in unstable intertrochanteric fractures using cerclage wire and lag screws: a comparative study. *Injury* 2017; **48** Suppl 2: S18-S22 [PMID: [28802415](#) DOI: [10.1016/S0020-1383\(17\)30489-8](#)]
  - 19 **Eberle S**, Gerber C, von Oldenburg G, Högel F, Augat P. A biomechanical evaluation of orthopaedic implants for hip fractures by finite element analysis and in-vitro tests. *Proc Inst Mech Eng H* 2010; **224**: 1141-1152 [PMID: [21138232](#) DOI: [10.1243/09544119JJEIM799](#)]
  - 20 **Goffin JM**, Pankaj P, Simpson AH, Seil R, Gerich TG. Does bone compaction around the helical blade of a proximal femoral nail anti-rotation (PFNA) decrease the risk of cut-out? *Bone Joint Res* 2013; **2**: 79-83 [PMID: [23673407](#) DOI: [10.1302/2046-3758.25.2000150](#)]
  - 21 **Bergmann G**, Deuretzbacher G, Heller M, Graichen F, Rohlmann A, Strauss J, Duda GN. Hip contact forces and gait patterns from routine activities. *J Biomech* 2001; **34**: 859-871 [PMID: [11410170](#) DOI: [10.1016/S0021-9290\(01\)00040-9](#)]
  - 22 **Bayle N**, Patel AS, Crisan D, Guo LJ, Hutin E, Weisz DJ, Moore ST, Gracies JM. Contribution of Step Length to Increase Walking and Turning Speed as a Marker of Parkinson's Disease Progression. *PLoS One* 2016; **11**: e0152469 [PMID: [27111531](#) DOI: [10.1371/journal.pone.0152469](#)]
  - 23 **Robinson PS**, Placide R, Soslowky LJ, Born CT. Mechanical strength of repairs of the hip piriformis tendon. *J Arthroplasty* 2004; **19**: 204-210 [PMID: [14973864](#) DOI: [10.1016/j.arth.2003.08.011](#)]
  - 24 **Taylor ME**, Tanner KE, Freeman MA, Yettram AL. Stress and strain distribution within the intact femur: compression or bending? *Med Eng Phys* 1996; **18**: 122-131 [PMID: [8673318](#) DOI: [10.1016/1350-4533\(95\)00031-3](#)]
  - 25 **Schneider E**, Michel MC, Genge M, Zuber K, Ganz R, Perren SM. Loads acting in an intramedullary nail during fracture healing in the human femur. *J Biomech* 2001; **34**: 849-857 [PMID: [11410169](#) DOI: [10.1016/S0021-9290\(01\)00037-9](#)]
  - 26 **Duda GN**, Schneider E, Chao EY. Internal forces and moments in the femur during walking. *J Biomech* 1997; **30**: 933-941 [PMID: [9302616](#) DOI: [10.1016/S0021-9290\(97\)00057-2](#)]
  - 27 **Papini M**, Zdero R, Schemitsch EH, Zalzal P. The biomechanics of human femurs in axial and torsional loading: comparison of finite element analysis, human cadaveric femurs, and synthetic femurs. *J Biomech Eng* 2007; **129**: 12-19 [PMID: [17227093](#) DOI: [10.1115/1.2401178](#)]
  - 28 **Perez JV**, Warwick DJ, Case CP, Bannister GC. Death after proximal femoral fracture--an autopsy study. *Injury* 1995; **26**: 237-240 [PMID: [7649622](#) DOI: [10.1016/0020-1383\(95\)90008-1](#)]
  - 29 **Goosen JH**, Mulder MC, Bongers KJ, Verheyen CC. High revision rate after treatment of femoral neck fractures with an optionally (un)cemented stem. *Arch Orthop Trauma Surg* 2009; **129**: 801-805 [PMID: [18626652](#) DOI: [10.1007/s00402-008-0697-4](#)]



Published by **Baishideng Publishing Group Inc**  
7041 Koll Center Parkway, Suite 160, Pleasanton, CA 94566, USA  
**Telephone:** +1-925-3991568  
**E-mail:** [bpgoffice@wjgnet.com](mailto:bpgoffice@wjgnet.com)  
**Help Desk:** <https://www.f6publishing.com/helpdesk>  
<https://www.wjgnet.com>

